Polymer 169 (2019) 131–137

Contents lists available at ScienceDirect

Polymer

journal homepage: www.elsevier.com/locate/polymer

FCC or HCP: The stable close-packed lattice of crystallographically equivalent spherical micelles in block copolymer/homopolymer blend

Li-Ting Chen[a], Chun-Yu Chen[b], Hsin-Lung Chen[a,*]

[a] Department of Chemical Engineering, National Tsing Hua University, Hsinchu, 30013, Taiwan
[b] National Synchrotron Radiation Research Center, Hsinchu, 300, Taiwan

HIGHLIGHTS

- Spherical micelles formed by block copolymers can pack into 3D ordered lattice.
- FCC and HCP are the two generic types of close-packed lattices.
- HCP is favored over FCC for micelles formed by block copolymer/homopolymer blend.
- Connectivity of octahedron voids in lattice prescribes the better stability of HCP.

ARTICLE INFO

Keywords:
Spherical micelle
Block copolymer
Blend
FCC
HCP

ABSTRACT

Spherical micelles formed by block copolymers (bcps) are soft colloids capable of packing into three-dimensionally ordered lattice. Although close-packed sphere structure has been predicted to exist over a narrow region in the phase diagram, it remains unclear whether face-centered cubic (FCC) or hexagonal close packed (HCP) lattice is the stable close packing symmetry for the crystallographically equivalent bcp micelles, as they are essentially degenerated. The present study explores the lattice structure organized by the spherical micelles in bcp/homopolymer blends after erasing the solvent history involved in the blend preparation. The facts that the FCC structure developed in the solvent-cast blend transformed into HCP on heating and HCP phase was formed upon cooling from the disordered micelle phase attest that HCP was the favored close-packed lattice over FCC. The better thermodynamic stability of HCP phase was attributed to the more extensive connectivity of the octahedron voids in the lattice, which prescribed a higher overall translational entropy of the homopolymer chains localized in the voids for space filling.

1. Introduction

Crystallization is a self-ordering process transforming the matter from the disordered liquid state to the crystalline state in which the building block packs in a three-dimensionally (3D) ordered lattice. Crystallization is prevalent and of great importance in both nature and technology and its associated building blocks range from microscopic objects such as atoms and molecules to mesoscopic objects such as colloidal particles.

Crystallization of colloidal particles leads to the lattice structures governed by the particle geometry and interparticle interaction potential. Close-packed lattices are the stable packing symmetries for hard spheres [1]. Face-centered cubic (FCC) and hexagonal close packed (HCP) lattice with *Fm3m* and $P6_3/mmc$ symmetry, respectively, are the two generic types of close-packed lattice for the crystallographically equivalent spheres (i.e., the spheres having the same size). The difference between them lies in the stacking sequence of the hexagonal close-packed layers (HCPLs) for building up the 3D lattice, where FCC and HCP lattices are constructed by ABCABC and ABABAB … sequence of stacking along (111) and (001) direction, respectively [2]. The free energy difference between these two lattice structures is extremely small for hard spheres, where the entropy of FCC per sphere was reported to be only $10^{-3} \sim 10^{-2} k_B$ higher than that of HCP [3–9]; consequently, FCC has been considered as the favored packing lattice over HCP for hard spheres [1,10–14].

Spherical micelles formed by the amphiphilic molecules such as surfactants and block copolymers (bcps) are soft colloids which also form 3D lattice structure at sufficiently high micelle concentration [15–19]. These colloids are soft because of the variability of their geometric characteristics such as size and shape as well as their packing

* Corresponding author.
E-mail address: hlchen@che.nthu.edu.tw (H.-L. Chen).

https://doi.org/10.1016/j.polymer.2019.02.041
Received 11 December 2018; Received in revised form 17 February 2019; Accepted 21 February 2019
Available online 21 February 2019
0032-3861/ © 2019 Elsevier Ltd. All rights reserved.

lattice with respect to the change of environmental condition. In the case of bcp, the spherical micelles can be formed by the pure bcp molecules in the melt, by the blend of bcp with homopolymer, and by the solution of bcp with low-molecular-weight selective solvent. One unique feature of the bcp micelle is its penetrable corona, where the coronas of the neighboring micelles are allowed to overlap with one another to minimize the conformational entropy loss arising from the packing frustration of the coronal block chains for attaining homogeneous matrix density equivalent to the inherent density of the matrix polymer [18]. According to the analysis of Thomas et al., the overlap of the micelle coronas favors body-centered cubic (BCC) lattice, because BCC packing minimizes the unfavorable deformation of the coronal blocks, as long as inter-micellar overlap is favored for attaining the matrix density [18]. Nevertheless, if the corona of each micelle can attain the uniform density by itself without significant entropic penalty, the micelle behaves like a hard sphere and close-packed lattices may become the favorable structure. By considering the geometries of the Wigner-Seitz cells, Imaizumi et al. also demonstrated that the packing frustration of the coronal blocks in BCC lattice was weaker than that associated with FCC packing [20].

It has been established both theoretically and experimentally that BCC is the dominant lattice structure for bcp spherical micelles; nevertheless, self-consistent mean-field theory has predicted the existence of close-packed sphere (CPS) phase over a very narrow region in the phase diagram of neat bcp [21]. Experimentally, the first CPS-forming neat bcp system was reported by Imaizumi et al., where an elastomeric triblock copolymer, poly(1,3-cyclohexadiene)-*block*-poly(ethylene-co-but-1-ene)-*block*-poly(1,3-cyclohexadiene), was found to exhibit FCC lattice, when the sample was subjected to a flow treatment at 493 K followed by an annealing at 473 K [20]. It was proposed that the applied external field brought the triblock system to the weak segregation limit which favored FCC packing of the spherical micelles. The subsequent thermal annealing released the residual strain and hence improved the structural order of the FCC lattice [20]. This study demonstrated the significance of external stress field and subsequent thermal annealing for generating CPS phase with good structural order in neat bcp. We have reported the coexistence of FCC and disordered micelle phase over the temperature window of only 4 K in the quiescent melt of a neat poly(ethylene oxide)-*block*-poly(1,4-butadiene) (PEO-*b*-PB) [19].

In the cases of the mixtures of bcp with homopolymer [22] and with low-molecular weight selective solvents [23], the window of CPS becomes broader because the homopolymer chains or the solvent molecules located in the micelle coronas can be distributed over the matrix phase for space filling, such that the need of inter-micellar overlap is relaxed.

The packing of the bcp micelles becomes an even more complex problem after the recent discovery of the Frank-Kasper phase, in which the micelles were tetrahedrally close-packed with all the interstices being tetrahedrons [24–31]. The unit cells of the tetrahedrally close-packed lattices contain a large number of spheres which may not be crystallographically equivalent in that they have slightly different sizes and shapes. The existence of the Frank-Kasper phases further attests the squashable nature of the bcp micelles for achieving the most efficient packing state with the lowest overall deformation free energy of the block chains.

The present study is centered on the crystallographically equivalent micelles of bcps, where FCC or HCP is the favored packing lattice in the CPS phase. It remains unclear whether FCC or HCP is the more stable packing symmetry for bcp systems. Similar to the hard colloid systems, these two lattice structures of bcp micelles were found to be nearly degenerated [32,33]; however, if the subtle difference in free energy is seriously considered, HCP is seemingly more stable than FCC for neat bcp and bcp/homopolymer blend according to the mean-field theories [22,32], which is different from the scenario of hard colloids.

The present study attempts to resolve the relative stability of FCC and HCP in the bcp/homopolymer blends. In the previous studies, we have disclosed the formation of FCC phase in the blend of a nearly symmetric PEO-*b*-PB and a PB homopolymer (h-PB), wherein PEO blocks formed spherical microdomains in the matrix phase composed of the homogeneous mixture of PB blocks and h-PB chains [34,35]. The blending between PEO-*b*-PB and h-PB was accomplished by solvent casting, and the spherical micelles in the as-cast blend were found to pack in FCC lattice. This FCC phase was however metastable, as it was developed at the late stage of solvent evaporation and got trapped into the bulk state after complete solvent removal. This “trapped FCC phase” transformed to BCC and then to the thermodynamically stable FCC phase at the elevated temperature on heating. The transition between the packing lattices was accessible only when the precursory structure existed due to the high entropic barrier involved [35]. Our previous results appeared to suggest that FCC was the favored packing symmetry over HCP in the temperature region where CPS phase was stable. Nevertheless, considering the close proximity between the free energy of FCC and that of HCP, nonequilibrium effect may play an important role in the selection of the close-packed lattice; it may hence be speculated that the trapped FCC phase developed from solvent casting served as the seed or precursor that directed the micelles in PEO-*b*-PB/h-PB blend to pack into FCC lattice at the elevated temperature where CPS phase was stable.

To circumvent the nonequilibrium effect arising from solvent history, the bcp system should be brought to the disordered state followed by cooling for re-assembly and re-ordering of the micelles. The present study re-examines the micelle ordering in the PEO-*b*-PB/h-PB blends, where the PEO-*b*-PB was blended with a h-PB with a lower molecular weight to reduce the order-disorder transition temperature, such that the disordered micelle phase was accessible before thermal degradation. Moreover, we also resolve the packing lattice of the PEO-rich blend formed by blending the PEO-*b*-PB with h-PEO to yield PB spherical domains in the matrix phase composed of the mixture of PEO blocks and h-PEO. It will be shown that HCP was the favored lattice structure over FCC in both PB-rich and PEO-rich blends.

2. Experimental section

The PEO-*b*-PB with the number average molecular weights (M_n) of PEO and PB block of 7.5×10^3 and 5.5×10^3 g/mol, respectively, was acquired from Polymer Source, Inc. Its polydispersity index (M_w/M_n) was 1.04. The 1,4-addition h-PB with $M_n = 1.0 \times 10^3$ g/mol and the h-PEO with $M_n = 1.5 \times 10^3$ g/mol were also obtained from Polymer Source, Inc. The molecular weight of the h-PB used here was about one half that ($M_n = 2.6 \times 10^3$) of the h-PB studied previously [35]. The blends with the overall volume fractions of PB (f_{PB}) or PEO (f_{PEO}) of 0.17 were prepared by solvent casting. The PEO-*b*-PB and the homopolymers were first dissolved in toluene at room temperature followed by drying in vacuo at 60 °C for 4 h to obtain the solvent-cast blends.

Temperature-dependent small angle X-ray scattering (SAXS) measurements were conducted at beamline BL23A1 of the National Synchrotron Radiation Research Center (NSRRC), Hsinchu, Taiwan. The energy of the employed monochromatic radiation was 15 keV, prescribing the X-ray wavelength of 0.83 Å. The 2D scattering patterns were collected with a Mar charge-coupled device (CCD) detector. The measured magnitude of the scattering wave vector q ranged from 0.07 to 4 nm^{-1} ($q = 4\pi/\lambda\ sin(\theta/2)$, where θ is the scattering angle and λ is the wavelength). All the scattering profiles were corrected for the scatterings from air and an empty cell. The temperature ramping rate was about 5 °C/min, and the sample was allowed to equilibrate at each temperature for five minutes followed by data acquisition for five minutes. All SAXS measurements were conducted under nitrogen atmosphere, which effectively circumvented the occurrence of degradation and crosslinking reaction.

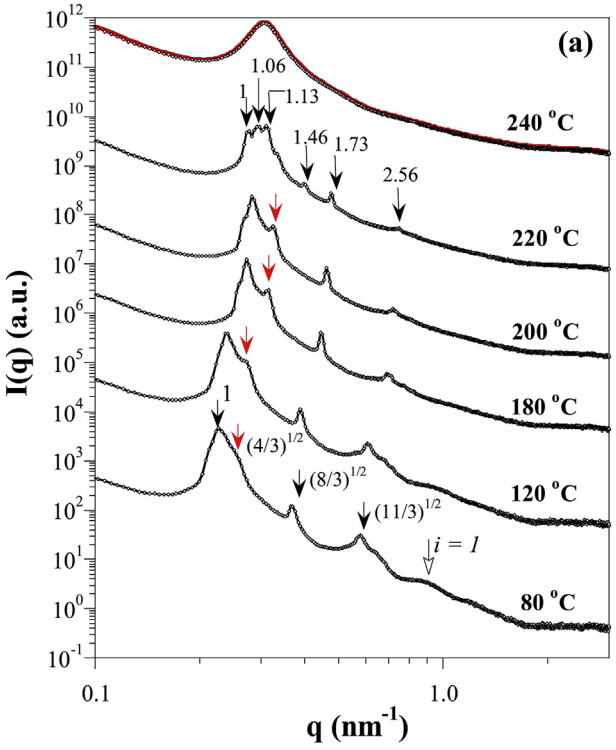

Fig. 1. Temperature-dependent SAXS profiles of PEO-*b*-PB/h-PB blend (f_{PEO} = 0.17) collected in a heating cycle. The temperatures are indicated in the figure. The $(4/3)^{1/2}$ peak marked by the red arrow became sharper with increasing temperature up to 200 °C. The solid curve superposing on the data of 240 °C is the fit by the Percus-Yevick model. (For interpretation of the references to colour in this figure legend, the reader is referred to the Web version of this article.)

3. Results and discussion

SAXS is a convenient tool for identifying the packing lattice of the spherical micelles of bcp. FCC lattice displays a series of diffraction peaks with the position ratio of 1: $(4/3)^{1/2}$: $(8/3)^{1/2}$: $(11/3)^{1/2}$: $(12/3)^{1/2}$, corresponding to (111), (200), (220), (311), (222) … diffraction, respectively, while an ideal HCP lattice with the ratio of the two lattice parameters c/a = 1.63 exhibits the peaks with the position ratio of 1: 1.06: 1.13: 1.46: 1.73 … associated with (100), (002), (101), (102), (110) diffractions, respectively.

Fig. 1 displays the temperature-dependent SAXS profiles of PEO-*b*-PB/h-PB blend collected in a heating cycle. The SAXS profile at 80 °C was found to display four peaks with the position ratio of 1: $(4/3)^{1/2}$: $(8/3)^{1/2}$: $(11/3)^{1/2}$. The broad peak marked by "$i=1$" was the first-order form factor maximum of the PEO spheres, which prescribed the average radius of the spheres of 10.8 nm. The observed scattering profile suggested the formation of FCC lattice; however, we noticed that, while the other three diffraction peaks were sharp, the $(4/3)^{1/2}$ peak was very broad. If the peak broadening were caused by lattice distortion and finite grain size, all the peaks instead of just one peak should have been broadened, as demonstrated by the calculated scattering profiles of FCC phase displayed in Fig. 2a. The scattering curves (i) and (ii) in Fig. 2a were calculated using the scattering function developed by Förster et al., which considered the effects of finite grain size, lattice distortion, and domain size distribution in formulating the analytical expressions for the scattering functions of various lattices [36]. Curve (i) was calculated using the following parameter values associated with FCC lattice: lattice constant = 47.9 nm, grain size = 100 nm, average sphere radius = 10.8 nm, and mean displacement of lattice points = 1 nm. Curve (ii) was calculated with the same parameter values except that the grain size was increased to 300 nm. Comparing scattering curve (i) and (ii), it can be seen that decreasing grain size broadened all diffraction peaks, which is different from the feature of the SAXS profile observed at 80 °C in Fig. 1.

We found that the scattering feature at 80 °C could be explained by considering the close stacking of the HCPLs in random sequence (e.g. ABCBCABAC.) rather than in the regular ABCABC sequence in FCC lattice [1]. Such a random stacking of HCPLs is denoted as "r-HCP" here. Curve (iii) in Fig. 2a was the calculated SAXS profile associated with the random close stacking of 22 HCPLs of monodisperse spheres. For the calculation, we first constructed the reference layer (i.e., the A layer) composed of 10 unit cells of the hexagonally packed mass points (corresponding to the centers of the spherical micelles) characterized by the hexagonal lattice vectors **a** and **b**. This reference layer was then used to construct the subsequent layers, where Layers B and C were obtained by a translation of $\mathbf{a}/3+2\mathbf{b}/3$ and $2\mathbf{a}/3+\mathbf{b}/3$ relative to the reference A layer, respectively [1]. In our assignment of stacking sequence, the neighboring layers must be closely stacked, that is, AA, BB, and CC sequences were prohibited. Upon designating the stacking sequence of HCPLs of the mass points, the lattice factor $S(q)$ of the constructed r-HCP phase was calculated by the Debye equation [37].

$$S(q) = \sum_i \sum_j \frac{\sin(q|\mathbf{r_i} - \mathbf{r_j}|)}{q|\mathbf{r_i} - \mathbf{r_j}|} \quad (1)$$

where $\boldsymbol{r_i}$ and $\boldsymbol{r_j}$ stand for the positions of the mass points in the lattice, and the summation in Eq. (1) was carried out over all mass points building up the r-HCP phase. Once $S(q)$ was obtained, the scattering intensity of the r-HCP phase was calculated by multiplying $S(q)$ with the form factor $P(q,R)$ of the monodisperse sphere with a designated radius R, viz. $I(q) = KS(q)P(q,R)$, where K is a proportionality constant.

Curve (iii) in Fig. 2a was obtained by averaging the intensity profiles of 100 randomly assigned r-HCP sequences for 22 layers with the interlayer spacing of 27.6 nm and R of 10.8 nm. It can be seen that the calculated SAXS curve at $q < 0.45\,nm^{-1}$ of the r-HCP phase agreed well with the observed scattering profile at 80 °C, as the $(4/3)^{1/2}$ peak appeared as a broad shoulder beside the primary peak, while the other peaks were sharp.

The $(4/3)^{1/2}$ peak became progressively sharper upon heating to 120–200 °C, showing the reorganization of the stacking sequence to generate the grains in which the spherical micelles packed in FCC lattice. The SAXS profile observed at 120 °C could indeed be simulated by the sum of the calculated scattering curve of r-HCP and FCC phase with the weighting factors of 0.7 and 0.3, respectively (Fig. 2b). The proportion of FCC phase increased to ca. 50% at 180 °C.

When the temperature was further raised to 220 °C, a totally different scattering profile was observed; now the positions of the diffraction peaks followed the ratio of 1: 1.06: 1.13: 1.46: 1.73 …, which was consistent with that prescribed by HCP lattice. The formation of HCP phase was further verified by the agreement between the observed SAXS profile and the calculated scattering curve of HCP lattice (to be demonstrated in Fig. 3b) [36]. It should be noted that the (102) peak in the observed SAXS profile appeared to be broader than (101) and (110) peaks, signaling the existence of a minor fraction of stacking fault in the HCP lattice.

The diffraction peaks vanished when the temperature was increased to 240 °C, at which the scattering curve was characterized by a broad halo at 0.31 nm^{-1} and a vague shoulder at 0.49 nm^{-1}. The fact that this SAXS profile could be fitted satisfactorily by the Percus-Yevick hard sphere model attested that the blend was in the disordered micelle phase, in which the spherical micelles only showed short-range order.

The temperature-dependent SAXS profiles revealed the transformation of the packing state of the spherical micelles formed in the solvent-cast blend upon heating. During the solvent evaporation, the micelles were able to form HCPL first, but the subsequent stacking of these layers occurred so rapidly that the communication of a given layer with those beyond the nearest neighbors could not proceed

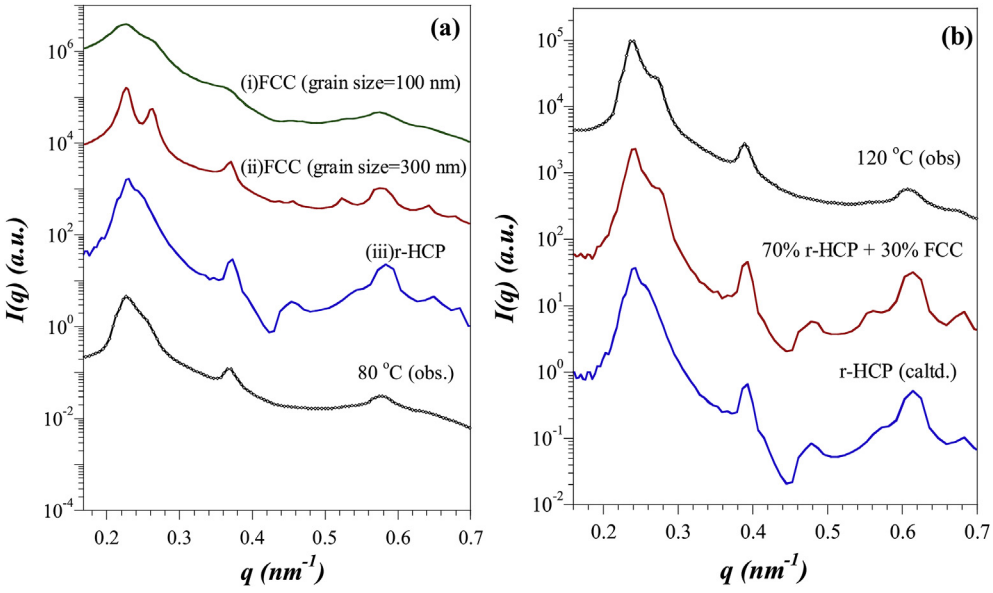

Fig. 2. (a) Comparison of the SAXS profile observed at 80 °C with the scattering curves calculated for FCC and r-HCP phase. Scattering curve (i) was calculated using the scattering function developed by Förster et al. [36], which considers the effects of finite grain size, lattice distortion, and domain size distribution in FCC lattice with the following parameter values: lattice constant = 47.9 nm, grain size = 100 nm, average sphere radius = 10.8 nm, and mean displacement of lattice points = 1 nm. Scattering curve (ii) was calculated by the same scattering function with the same parameter values except that the grain size was increased to 300 nm. Scattering curve (iii) associated with r-HCP structure was calculated by assuming the random close stacking of 22 HCPLs with the interlayer distance of 27.6 nm without considering sphere size distribution and lattice distortion. Scattering curves (i) and (ii) demonstrated that all diffraction peaks broadened with decreasing grain size. The observed scattering profile at $q < 0.45\,nm^{-1}$ is seen to agree well with that associated with r-HCP structure. (b) Comparison of the SAXS profile observed at 120 °C with the scattering curves calculated for r-HCP phase and by the sum of the scattering profiles of r-HCP and FCC phase with the weighting factor of 0.7 and 0.3, respectively. The observed SAXS profile at $q < 0.45\,nm^{-1}$ agrees with that prescribed by the coexistence of the two structures.

effectively in time, thereby leading to random close stacking of the HCPLs. The nonequilibrium random sequence gradually reorganized into ABCABC sequence to construct FCC lattice upon heating up to 200 °C. However, the FCC packing became unstable and transformed into HCP as the temperature was further raised to 220 °C. The disordered micelle phase was eventually accessed at 240 °C. The experimental results suggested that HCP was thermodynamically more stable than FCC, and the observed FCC phase was an intermediate structure in the kinetic pathway of the transformation from r-HCP to HCP phase. Fig. S1 of the Supplementary Materials shows the temperature dependence of the lattice constants associated with FCC and HCP phases, which demonstrated that the lattice constants decreased with increasing temperature due to the reduction of the segregation strength.

Since the micelle ordering relevant to the solvent history was erased at 240 °C, the blend was subsequently cooled to allow the micelle to attain the stable packing lattice via ordering from the disordered micelle phase. Fig. 3 displays the temperature-dependent SAXS profiles collected in the cooling cycle. Interestingly, when the blend was cooled from 240 to 200 °C, the scattering pattern associated with the HCP lattice emerged, where the SAXS profile observed at 200 °C agreed well with that calculated for HCP lattice with the lattice parameters of $a = 27$ nm and $c = 44.0$ nm and the average sphere radius of 8.0 nm (see Fig. 3b). The result demonstrated the thermal reversibility of the transition between HCP and disordered micelle phase. Nevertheless, the FCC phase observed in the original heating cycle was not recovered upon further cooling, implying that it was metastable in nature. Although HCP phase remained stable throughout the entire temperature range below 240 °C, the associated diffraction peaks broadened with decreasing temperature, which may be attributed to the reorganization of the micelle structure in the lattice by increasing the association number in response to the increase of χ.

Fig. S3 in the Supplementary Materials shows the average radius of PEO spherical domain as a function of temperature. Similar to the lattice constant, the average sphere radius decreased with increasing

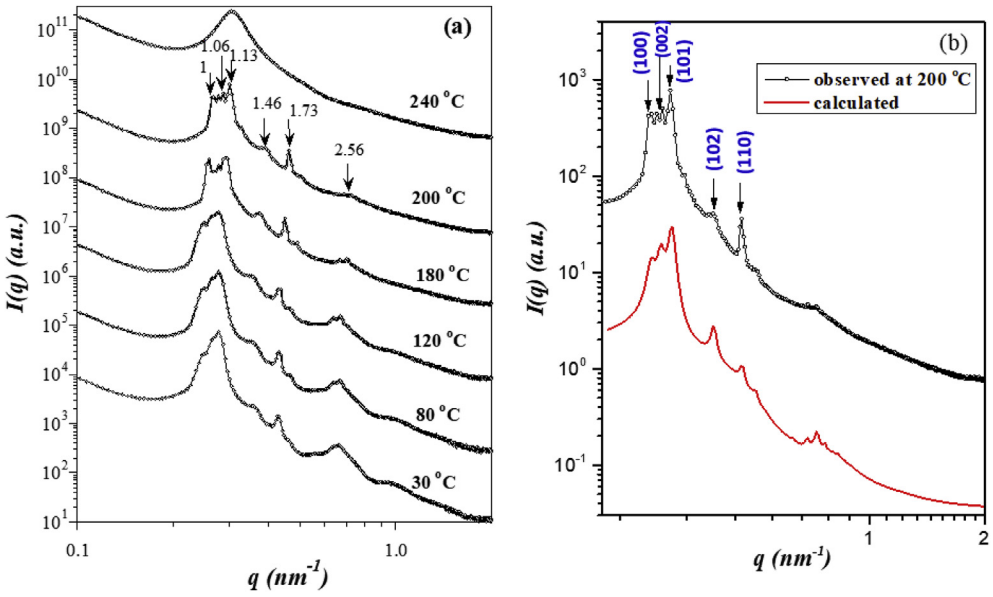

Fig. 3. (a) Temperature-dependent SAXS profiles of PEO-*b*-PB/h-PB blend ($f_{PEO} = 0.17$) collected in a cooling cycle after reaching the disordered micelle phase at 240 °C. The temperatures are indicated in the figure. (b) Comparison between the SAXS profile observed at 200 °C and that calculated by the scattering function developed by Förster et al. [36] with the following parameter values for HCP lattice: the lattice parameters $a = 27$ nm and $c = 44.0$ nm, and the average sphere radius = 8.0 nm. The sphere radius determined by SAXS agreed well with that determined by the TEM micrograph shown in Fig. S5 of the Supplementary Materials.

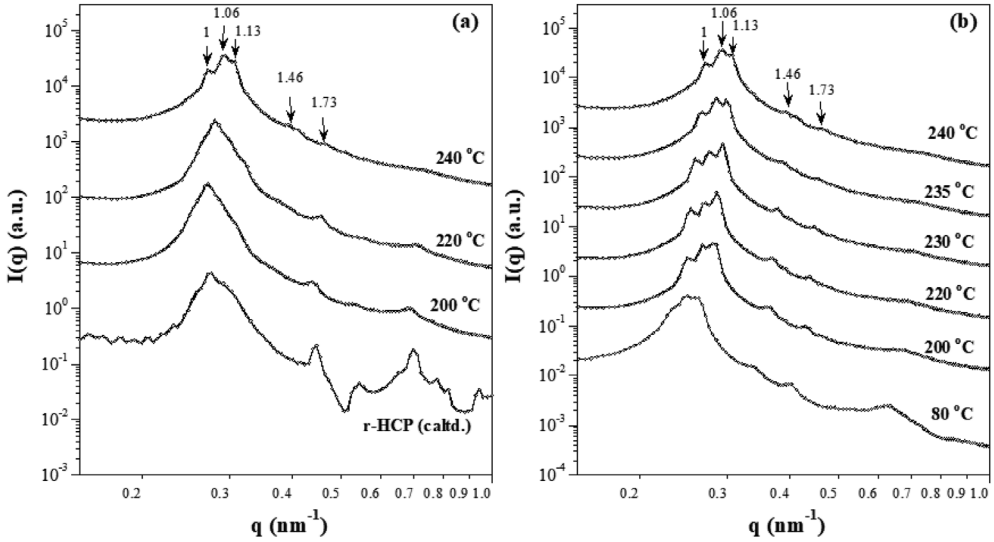

Fig. 4. Temperature-dependent SAXS profiles of the PEO-*b*-PB/h-PEO (f_{PB} = 0.17) blend collected in a (a) heating cycle and (b) subsequent cooling cycle. The scattering profile associated with r-HCP phase is display in (a) to demonstrate that the solvent-cast blend showed such a morphology below 240 °C.

temperature, since the lower interfacial free energy at the higher temperature allowed the spherical domains to increase their surface area-to-volume ratio by decreasing the domain size for relaxing the stretching of coronal blocks. It is noted that the domain size of HCP phase was smaller than that associated with the FCC phase under a given temperature, which may be attributed to the fact that FCC phase was metastable whereas HCP was the thermodynamically stable structure; in this case, the association number of the spherical micelles in FCC phase did not correspond to the equilibrium value.

Our SAXS results disclosed that the FCC phase developed in the solvent-cast blend transformed into HCP phase on heating and, upon removing the solvent history, HCP instead of FCC phase was formed from the disordered micelle phase. Both phase transition processes attested that HCP was a more stable packing symmetry than FCC for the spherical micelles formed in bcp/homopolymer blends. To consolidate this postulate, we further explored the packing lattice in the PEO-rich blend formed by blending the PEO-*b*-PB with h-PEO; in this case, the micelle is composed of the core assembled by PB blocks and the corona containing the mixture of PEO blocks and h-PEO. Fig. 4a and Fig. 4b display the temperature-dependent SAXS profiles of the PEO-*b*-PB/h-PEO blend collected in a heating and subsequent cooling cycle, respectively. Upon heating the solvent-cast blend to 200–220 °C, the scattering patterns were consistent with that prescribed by the r-HCP phase, as demonstrated in Fig. 4a. When the temperature was further increased to 240 °C, a series of diffraction peaks with the position ratio associated with HCP lattice were identified, showing that the structure transformed into HCP phase. The disordered micelle phase was not accessible before the occurrence of thermal degradation for this blend; therefore, the system was cooled from the HCP phase developed at 240 °C. It can be seen in Fig. 4b that HCP phase remained stable throughout the cooling process till 30 °C, at which the crystallization of PEO in the matrix phase disrupted the structure formed from microphase separation. The experimental results of the PEO-rich blend supported the postulate that, as long as CPS was the thermodynamically stable structure, HCP was a more favored packing lattice than FCC for the spherical micelles in bcp/homopolymer blends.

The better stability of HCP than FCC appeared to conflict with the previous studies showing that FCC is the favored packing lattice over HCP for hard spheres. Recently, a theoretical work by Mahynski et al. demonstrated that the addition of linear homopolymers can thermodynamically bias the crystallization of hard-sphere colloids to produce HCP structure over FCC [38,39]. This intriguing phenomenon is entropically driven and is governed by the spatial arrangement of the interstices in the close-packed lattices. Although both FCC and HCP have the same packing fraction of 0.74, the arrangements of the voids that account for the remaining volume fraction in the lattices are different. There are two types of voids in both lattices, i.e., tetrahedron void (TV) and octahedron void (OV), as schematically illustrated in Fig. 5a. In FCC structure, the arrangement of the voids along the stacking direction of HCPLs always follows the sequence of … TV-OV-TV-OV-TV …, and each OV is capped by the two TVs adjacent to it, as schematically illustrated in Fig. 5b [38,39]. In the case of HCP lattice, OVs and TVs situate directly on top of themselves owing to the ABAB … stacking, generating OV and TV columns separately along the close stacking direction, as illustrated in Fig. 5c. In this case, while a pair of adjacent TVs are end-capped by themselves in a given TV column, the OVs in each OV column are interconnected and form an opened channel [38,39]. When a sufficiently long polymer chain is added into the lattice of the hard-sphere colloids, it can spread itself across neighboring OVs in HCP, whereas it would be confined into an OV-TV pair in FCC; therefore, the polymer chain has a higher entropy in HCP lattice, and once this effect is sufficiently dominant, HCP becomes the favored packing structure over FCC even for the hard colloids [38,39].

Here we extend such a concept to explain why HCP lattice was more favored than FCC for the close packing of spherical micelles formed by bcp/homopolymer blends. The fact that the spherical micelles studied here adopted close packing implied that they behaved like hard spheres without significant overlap of their coronas. In this case, the voids in the closely packed lattice are filled either by the coronal block chains or by the homopolymer. If this is accomplished by the coronal blocks, those block chains reaching the void regions will have to stretch more than the others, and hence lose conformational entropy. Such an entropic penalty can be released if the voids are alternatively filled by the homopolymer chains. For the homopolymer chains localized into the voids, the space available for them to explore in the lattice determines their translational entropy. In HCP lattice, the hompolymer chains located in the OVs enjoy higher translational entropy because the channels formed by the long-range connectivity of the OVs provides a continuous space for them to explore. The translational degree of freedom of homopolymer in FCC lattice is slightly more restricted, as the OVs are always capped by the adjacent TVs. On basis of this argument, we postulate that HCP is an entropically favored lattice over FCC for the packing of spherical micelles of bcp/homopolymer blends.

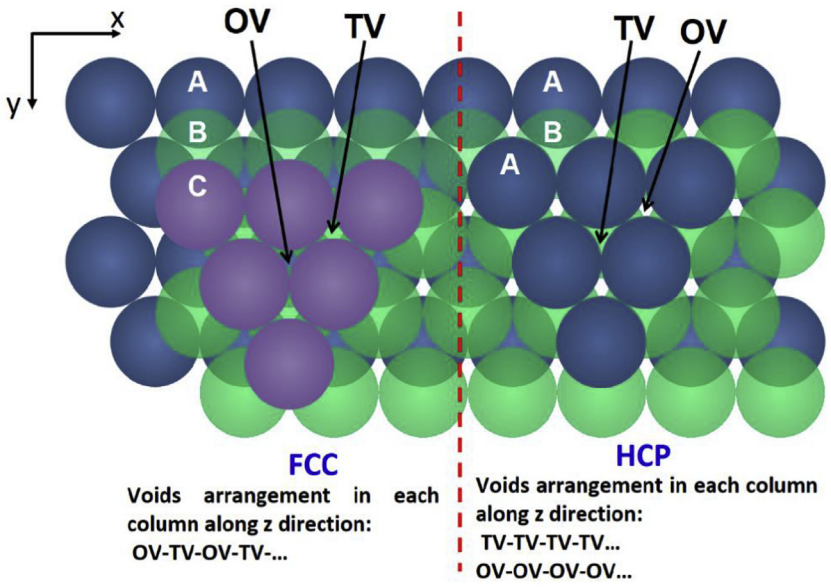

Fig. 5. (a) Schematic illustration of the stacking of HCPLs in FCC and HCP lattice, generating tetrahedron void (TV) and octahedron void (OV). The spatial organizations of these two types of voids along the close stacking direction are different in the two lattices. The voids organize in the sequence of TV-OV-TV-OV … in FCC lattice with each OV capped by the two TVs adjacent to it, as shown in (b). In HCP phase, OVs and TVs situate directly on top of themselves, generating OV and TV columns separately along the close stacking direction, as illustrated in (c).

4. Conclusions

In conclusion, the present study explores the stable close-packed lattice of the crystallographically equivalent spherical micelles formed by the blends of block copolymer and the corresponding homopolymer by studying the lattice structure formed after removing the solvent history involved in blend preparation. In the as-cast PEO-*b*-PB/h-PB blend, the HCPLs organized by the spherical micelles showed random close stacking, but the random sequence tended to reorganize into ABCABC … sequence constructing the FCC lattice upon heating. The FCC structure however transformed into HCP before the disordered micelle phase was accessed at high temperature. HCP phase was found to develop from the disordered micelle phase upon subsequent cooling, and this lattice structure persisted throughout the entire temperature range in the cooling process, indicating that HCP was the more stable packing lattice than FCC. HCP phase was also found for the PEO-*b*-PB/h-PEO blend. The better thermodynamic stability of HCP was attributed to the higher translational entropy of the homopolymer chains localized into the OVs due to the extended connectivity of these voids in the lattice.

Acknowledgment

H.-L. Chen would like to thank Professor Takeji Hashimoto for his mentorship and friendship over the past 19 years. The CPS phase of PEO-*b*-PB system was discovered during HLC's visit to Professor Hashimoto's laboratory at Kyoto University in 2001. The present work is supported by the Ministry of Science and Technology (MOST) under

grant No. MOST102-2221-E-007-136-MY3. The authors appreciate the beamtime of BL23A provided by NSRRC in Taiwan.

Appendix A. Supplementary data

Supplementary data to this article can be found online at https://doi.org/10.1016/j.polymer.2019.02.041.

References

[1] P.N. Pusey, W. van Megen, P. Bartlett, B.J. Ackerson, J.G. Rarity, S.M. Underwood, Structure of crystals of hard colloidal spheres, Phys. Rev. Lett. 63 (1989) 2753–2756 https://doi.org/10.1103/PhysRevLett.63.2753.

[2] C. Kittel, Introduction to Solid State Physics, eighth ed., Wiley, New York, 2004.

[3] K.W. Kratky, The stability of fcc and hcp hard-sphere crystals, Chem. Phys. 57 (1981) 167–174 https://doi.org/10.1016/0301-0104(81)80031-6.

[4] P.G. Bolhuis, D. Frenkel, S.C. Mau, D.A. Huse, Entropy difference between crystal phases, Nature 388 (1997) 235–236 http://doi.org/10.1038/40779.

[5] S.C. Mau, D.A. Huse, Stacking entropy of hard-sphere crystals, Phys. Rev. E 59 (1999) 4396–4401 https://doi.org/10.1103/PhysRevE.59.4396.

[6] A.D. Bruce, N.B. Wilding, G.J. Ackland, Free energy of crystalline solids: a lattice-switch Monte Carlo method, Phys. Rev. Lett. 79 (1997) 3002–3005 https://doi.org/10.1103/PhysRevLett.79.3002.

[7] A.D. Bruce, A.N. Jackson, G.J. Ackland, N.B. Wilding, Lattice-switch monte carlo method, Phys. Rev. E, Stat. Nonlinear, Phys. Rev. E 61 (2000) 906–919 https://doi.org/10.1103/PhysRevE.61.906.

[8] L.V. Woodcock, Entropy difference between the face-centred cubic and hexagonal close-packed crystal structures, Nature 385 (1997) 141–143 https://doi.org/10.1038/385141a0.

[9] L.V. Woodcock, Reply: Entropy difference between crystal phases, Nature 388 (1997) 236–237 https://doi.org/10.1038/40781.

[10] S. Pronk, D. Frenkel, Can stacking faults in hard-sphere crystals anneal out spontaneously? J. Chem. Phys. 110 (1999) 4589–4592 https://doi.org/10.1063/1.478339.

[11] M.S. Elliot, S.B. Haddon, W.C.K. Poon, Direct observation of pre-critical nuclei in a metastable hard-sphere fluid, J. Phys. Condens. Matter 13 (2001) 553–558 https://doi.org/10.1088/0953-8984/13/23/104.

[12] S. Heitkam, W. Drenckhan, J. Fröhlich, Packing spheres tightly: Influence of mechanical stability on close-packed sphere structures, Phys. Rev. Lett. 108 (2012) 148302 https://doi.org/10.1103/PhysRevLett.108.148302.

[13] A. van der Net, W. Drenckhan, D. Weaire, S. Hutzler, The crystal structure of bubbles in the wet foam limit, Soft Matter 2 (2006) 129–134 https://doi.org/10.1039/b515537a.

[14] A. van der Net, G.W. Delaney, W. Drenckhan, D. Weaire, S. Hutzler, Crystalline arrangements of microbubbles in monodisperse foams, Colloids Surfaces A Physicochem. Eng. Asp. 309 (2007) 117–124 https://doi.org/10.1016/j.colsurfa.2006.11.056.

[15] I.W. Hamley, C. Daniel, W. Mingvanish, S.M. Mai, C. Booth, L. Messe, A.J. Ryan, From hard spheres to soft spheres: the effect of copolymer composition on the structure of micellar cubic phases formed by diblock copolymers in aqueous solution, Langmuir 16 (2000) 2508–2514 https://doi.org/10.1021/la991035j.

[16] X.B. Zeng, Y.S. Liu, M. Impéror-Clerc, Hexagonal close packing of nonionic surfactant micelles in water, J. Phys. Chem. B 111 (2007) 5174–5179 https://doi.org/10.1021/jp0687955.

[17] M. Imai, I. Yoshida, T. Iwaki, K. Nakaya, Static and dynamic structures of spherical nonionic surfactant micelles during the disorder-order transition, J. Chem. Phys. 122 (2005) 044906https://doi.org/10.1063/1.1839559.

[18] E.L. Thomas, D.J. Kinning, D.B. Alward, C.S. Henkee, Ordered packing arrangements of spherical micelles of diblock copolymers in two and three dimensions, Macromolecules 20 (1987) 2934–2939 https://doi.org/10.1021/ma00177a049.

[19] Y.Y. Huang, J.Y. Hsu, H.L. Chen, T. Hashimoto, Existence of fcc-packed spherical micelles in diblock copolymer melt, Macromolecules 40 (2007) 406–409 https://doi.org/10.1021/ma062149m.

[20] K. Imaizumi, T. Ono, T. Kota, S. Okamoto, S. Sakurai, Transformation of cubic symmetry for spherical microdomains from face-centred to body-centred cubic upon uniaxial elongation in an elastomeric triblock copolymer, J. Appl. Crystallogr. 36 (2003) 976–981 https://doi.org/10.1107/S0021889803008471.

[21] M.W. Matsen, F.S. Bates, Unifying weak-and strong-segregation block copolymer theories, Macromolecules 29 (1996) 1091–1098 https://doi.org/10.1021/ma951138i.

[22] M.W. Matsen, Stabilizing new morphologies by blending homopolymer with block copolymer, Phys. Rev. Lett. 74 (1995) 4225–4228 https://doi.org/10.1103/PhysRevLett.74.4225.

[23] T.P. Lodge, B. Pudil, K.J. Hanley, The full phase behavior for block copolymers in solvents of varying selectivity, Macromolecules 35 (2002) 4707–4717 https://doi.org/10.1021/ma0200975.

[24] T.M. Gillard, S. Lee, F.S. Bates, Dodecagonal quasicrystalline order in a diblock copolymer melt, Proc. Natl. Acad. Sci. Unit. States Am. 113 (2016) 5167–5172 https://doi.org/10.1073/pnas.1601692113.

[25] K. Kim, M.W. Schulze, A. Arora, R.M. Lewis, M.A. Hillmyer, K.D. Dorfman, F.S. Bates, Thermal processing of diblock copolymer melts mimics metallurgy, Science 356 (2017) 520–523 https://doi.org/10.1126/science.aam7212.

[26] S. Lee, M.J. Bluemle, F.S. Bates, Discovery of a frank-Kasper s phase in sphere-forming block copolymer melts, Science 330 (2010) 349–353 https://doi.org/10.1126/science.1195552.

[27] S. Lee, C. Leighton, F.S. Bates, Sphericity and symmetry breaking in the formation of Frank–Kasper phases from one component materials, Proc. Natl. Acad. Sci. Unit. States Am. 111 (2014) 17723–17731 https://doi.org/10.1073/pnas.1408678111.

[28] H. Takagi, R. Hashimoto, N. Igarashi, S. Kishimoto, K. Yamamoto, Frank–Kasper σ phase in polybutadiene-poly(ε- caprolactone) diblock copolymerpolybutadiene blends, J. Phys. Condens. Matter Pap. 29 (2017) 204002 https://doi.org/10.1088/1361-648X/aa6908.

[29] W.H. Li, C. Duan, A.C. Shi, Nonclassical Spherical Packing Phases Self-Assembled from AB-Type Block Copolymers, ACS Macro Lett. 6 (2017) 1257–1262 https://doi.org/10.1021/acsmacrolett.7b00756.

[30] M. Liu, Y.C. Qiang, W.H. Li, F. Qiu, A.C. Shi, Stabilizing the Frank-Kasper phases via binary blends of AB diblock copolymers, ACS Macro Lett. 5 (2016) 1167–1171 https://doi.org/10.1021/acsmacrolett.6b00685.

[31] N. Xie, W.H. Li, F. Qiu, A.C. Shi, σ Phase formed in conformationally asymmetric AB-type block copolymers, ACS Macro Lett. 3 (2014) 906–910 https://doi.org/10.1021/mz500445v.

[32] M.W. Matsen, Phase behavior of block copolymer/homopolymer blends, Macromolecules 28 (1995) 5765–5773 https://doi.org/10.1021/ma00121a011.

[33] M.W. Matsen, Fast and accurate SCFT calculations for periodic block-copolymer morphologies using the spectral method with Anderson mixing, Eur. Phys. J. E 30 (2009) 361–369 https://doi.org/10.1140/epje/i2009-10534-3.

[34] Y.Y. Huang, H.L. Chen, T. Hashimoto, Face-centered cubic lattice of spherical micelles in block copolymer/homopolymer blends, Macromolecules 36 (2003) 764–770 https://doi.org/10.1021/ma0204305.

[35] Y.Y. Huang, J.Y. Hsu, H.L. Chen, T. Hashimoto, Precursor-driven bcc-fcc order-order transition of sphere-forming block copolymer/homopolymer blend, Macromolecules 40 (2007) 3700–3707 https://doi.org/10.1021/ma070066f.

[36] S. Förster, A. Timmann, M. Konrad, C. Schellbach, A. Meyer, S.S. Funari, P. Mulvaney, R. Knott, Scattering curves of ordered mesoscopic materials, J. Phys. Chem. B 109 (2005) 1347–1360 https://doi.org/10.1021/jp0467494.

[37] P. Debye, X-ray dispersal, Ann. Phys. 46 (1915) 809–823.

[38] N.A. Mahynski, A.Z. Panagiotopoulos, D. Meng, S.K. Kumar, Stabilizing colloidal crystals by leveraging void distributions, Nat. Commun. 5 (2014) 4472 https://doi.org/10.1038/ncomms5472.

[39] N.A. Mahynski, S.K. Kumar, A.Z. Panagiotopoulos, Relative stability of the FCC and HCP polymorphs with interacting polymers, Soft Matter 11 (2015) 280–289 https://doi.org/10.1039/c4sm02191f.